Geology and Lithogeochemistry of the Supracrustal Sequence and Interlayered Metabasites of NE Santos Dumont Region (MG)
Geologia e Litogeoquímica da Sequência Supracrustal e
Metabasitos Intercalados da Região NE de Santos Dumont (MG)

Renata Hiraga[1,2]; José Renato Nogueira[2]; Beatriz Paschoal Duarte[2];
Claudia Sayão Valladares[2]; Vinicius de Oliveira Monteiro Guimarães[2] & Rodrigo Peternel[2]

[1]*Centro de Tecnologia Mineral, Av. Pedro Calmon, 900, 21941-908, Cidade Universitária, Rio de Janeiro, RJ, Brazil.*
[2]*Universidade do Estado do Rio de Janeiro, Faculdade de Geologia, Departamento de Geologia Regional e Geotectônica,
Rua São Francisco Xavier, 524, sala 4006, 20550-900, Maracanã, Rio de Janeiro, RJ, Brazil.*
*E-mails: renatahvc@yahoo.com.br; jrnog@gmail.com; biapasch@gmail.com;
claudia.s.valladares@gmail.com; vdomg@hotmail.com; rpeternel@gmail.com*

Abstract

The region near Santos Dumont town consists of a sequence of interlayered metabasic rocks and supracrustal gneisses. Two lithological units were individualized based on geological-structural mapping (1:50,000), petrography and lithogeochemistry: a metasedimentary sequence interlayered with metavolcanic rocks (Conceição do Formoso Group), and a group of metabasic rocks (Oliveira Fortes Unit). The metavolcanic sequence is represented by gneisses of dacitic and riolitic compositions, with calc-alkaline affinity and weak peraluminous character, suggesting that the original magma was contaminated by crustal component. These gneisses have a geochemical signature of a destructive margin environment and their origin can be related to volcanic arc magmatism. The metabasic rocks present geochemical signature of intraplate tholeiitic basalts and are interpreted as sills interlayered within the metavolcanosedimentary sequence.
Keywords: lithogeochemistry; geology; metabasites; supracrustal sequence

Resumo

A região próxima à cidade de Santos Dumont é constituída por uma sequência gnáissica supracrustal intercalada com rochas metabásicas. Duas unidades litológicas puderam ser individualizadas baseando-se no mapeamento geológico estrutural (1:50.000), petrografia e litogeoquímica: uma sequência metassedimentar intercalada com rochas metavulcânicas (Grupo Conceição do Formoso), e um grupo de rochas metabásicas (unidade Oliveira Fortes). A sequência metavulcânica é representada por gnaisses de composição dacítica a riolítica, com filiação cálcio alcalina e caráter levemente peraluminoso, sugerindo que o magma original foi contaminado por um componente crustal. Esses gnaisses tem uma assinatura geoquímica de margem destrutiva e sua origem pode ser relacionada à ambientes de arcos vulcânicos. As rochas metabásicas apresentam assinatura geoquímica de basaltos intraplaca toleíticos intraplaca, interpretados como *sills* alojados na sequência metavulcanossedimentar.
Palavras-chave: litogeoquímica; geologia; metabasitos; sequência supracrustal

1 Introduction

Santos Dumont region, situated in the southeastern portion of Minas Gerais State, can be considered as a key area to unravel the tectonic evolution of Araçuaí and Ribeira belts. The area can be located within the Mantiqueira Province (Almeida *et al.*, 1977, 1981), near the SSE boundary of the São Francisco Craton and raises different interpretations of its tectonic position. The tectonic and temporal relations, the boundary position and the interference zones between the Ribeira and Araçuaí belts, as well as the relation to the São Francisco Craton, are not well established and is still an open subject of discussion. The study area is considered part of the Autochthonous Tectonic Domain (ATD) of the Ribeira Belt (Heilbron *et al.,* 2004) and also can be included in the External Domain of the Araçuaí Belt (Pedrosa-Soares & Wiedemann-Leonardos, 2000). In a different interpretation, Trouw *et al.* (2013) insert the region in the southernmost portion of the Araçuaí Belt limited to the south by the Brasília belt.

The existence of open to tight folding, associated with NE-SW low angle ductile shear zones characterize its position on the external portion of the Ribeira Belt. These shear zones show a near down-dip stretching lineation coeval to the Ribeira belt deformation and deflect a NNW-SSE low angle foliation, with open folds and NE-SW gently limbs, related to the Araçuaí Belt structures.

To the south of the thrust boundary (Figure 1, geological map of the area), granitic to tonalitic orthogneisses, which can be correlated to the Mantiqueira Complex (Brandalise *et al.,* 1991b), occur as basement rocks to supracrustal sequences interlayered with metabasites of unknown age. To the north of this thrust boundary, no basement associations were found and rocks consists of thick sequences of gneisses of different origins (Conceição do Formoso Group) interlayered with centimetric to hectometric (1cm to 100 m) metabasite bodies (Oliveira Fortes Unit), metamorphosed under amphibolite facies conditions. The area to the north of the thrust boundary is the focus of this work.

On the basis of geological mapping, detailed petrographic and lithogeochemical data, this work focuses on the study of Conceição do Formoso Group and Oliveira Fortes Unit in order to approach geological and petrological evolution. This work also leads to regional correlations, adding data to broader discussions on tectonic models of the Araçuaí and Ribeira belts.

2 Materials and Methods

Petrological and structural studies are product of compilation of previous works, in addition to semi-detailed geological mapping (1:50000) and the description of 66 thin sections from 523 visited outcrops.

The lithogeochemical analysis was performed in two stages: samples were prepared at the LGPA (Laboratório Geológico de Processamento de Amostras, at the Universidade do Estado do Rio de Janeiro - UERJ); and analyzed at the Activation Laboratories Ltd. (Actlabs /Canada). ICP/AES (Inductively Coupled Plasma – Atomic Emission Spectrometry) was used to analyze the major elements, while ICP/MS (Inductively Coupled Plasma – Mass Spectrometry) was used for obtaining the trace elements and the REE, following the procedures proposed by Hoffman (1992). The detection limit ranges from 0,1 ppm (for La, Ce and Nd) to 30 ppm (Zn) and from 0,04 ppm to 0,05 ppm for the remaining trace and rare earth elements.

3 Geological Units

Santos Dumont area is characterized by a supracrustal sequence interlayered with metabasic rocks in several scales (Figure 1). The supracrustal sequence, here named as Conceição do Formoso Group, could be subdivided into two main lithological units, which cannot be individualized in map scale (1:50,000); one with homogeneous gneisses (biotite leucogneiss and hornblende-biotite gneiss) of possible igneous protolith and the other represented by heterogeneous paragneisses.

The first is composed of a homogenous biotite leucogneiss, which includes layers of (hornblende)-biotite gneiss. The paragneisses are heterogeneous biotite gneiss with variable content of muscovite, garnet and sillimanite, and lenses of gondites, cherts and quartzites.

The intrusive metabasic rocks of Oliveira Fortes Unit occur as lenses interlayered with the whole sequence (Figure 2) and exhibit preserved subophitic textures in garnet metagabbros and,
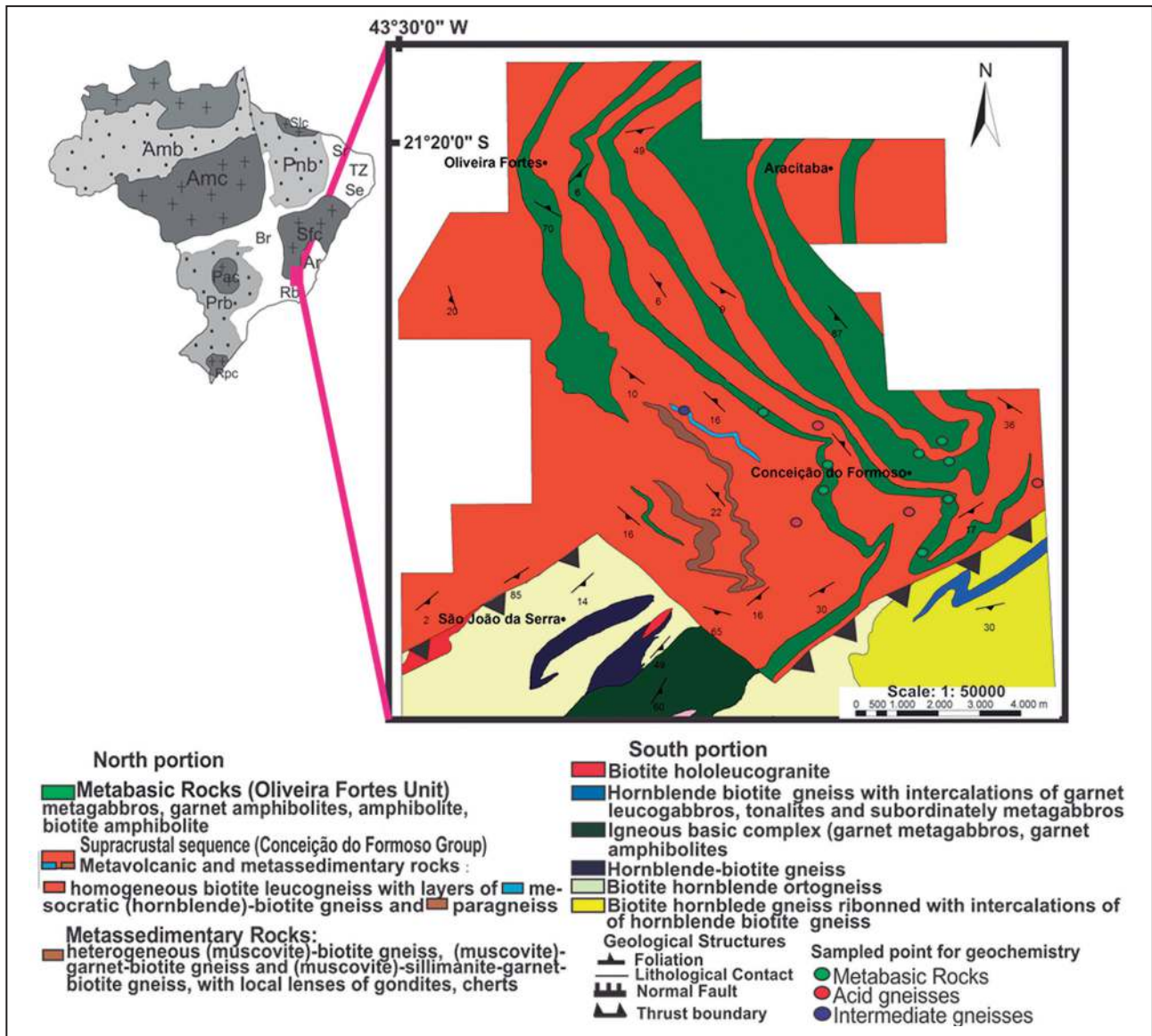
Figure 1 Geological map of Santos Dumont area and the schematic map showing the Santo Dumont area's location. Legend: Amb- Amazon basin; Prb-Paraná basin; Pnb- Parnaíba basin; Amc- Amazon craton; Pac- Paranapanema craton; Rpc- Rio de la Plata Craton; Sfc- São Francisco Craton; Slc- São Luis Craton; Br- Brasília belt; Rb- Ribeira belt; Ar- Araçuaí belt; Se- Sergipana belt ; TZ- Transversal Zone; Sr- Seridó belt.

subordinately, in metagabbros. In high deformed areas, petrographic compositions vary from garnet amphibolites and amphibolites to biotite amphibolites within the thrust zone.

The homogeneous biotite leucogneiss is fine-grained and characterized by equigranular texture and schistosity followed by the orientation of millimetric to submillimetric biotite-muscovite crystals. Its mineralogical composition is given by variables quantities of quartz (16-42%), microcline (13-52%), plagioclase (8-30%), biotite (14-22%) and muscovite (0-3%), with zircon and opaque minerals (~2) as accessories. Locally, exhibits relict euhedral to subhedral phenocrysts of microcline (Figure 3), with a degree of alteration characteristically superior as compared to the granoblastic matrix. These textural features together with its granitic composition, the abundance in microcline, the usual homogenous aspect, the fine grained texture with individual crystals of biotite and its form of occurrence in outcrops, sometimes representing thick homogeneous sequences over large areas, suggest the hypothesis that it might represent a sequence of rhyolitic volcanism, possibly associated to pyroclastic flow deposits and acid tuffs.

Also are present interdigitations of homoge-

Figure 2 Biotite leucogneiss (Bt-lgn) from Conceição do Formoso group; note the interlayered metabasic (Mb) rock in a homogeneous gneiss sequence.
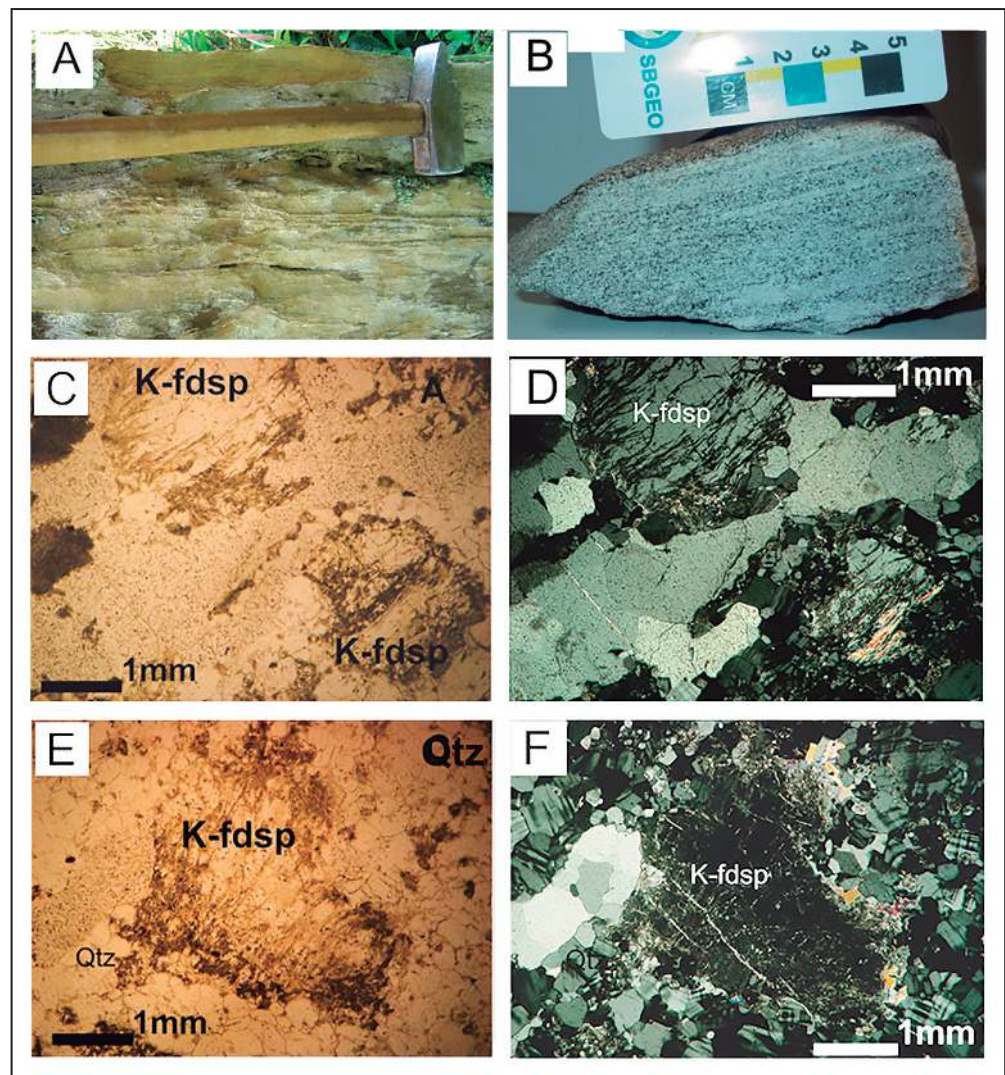

Figure 3 Aspects of the biotite leucogneiss. A. close outcrop view; B. hand sample with leucocratic and homogeneous aspect; C-F Granoblastic textured of homogeneous biotite leucogneiss showing euedric to subedric microcline (K-fdsp) phenocrysts. Figures C and E under parallel nicols. d and f under crossed polars. Legend: Qtz – quartz.

neous mesocratic (hornblende)-biotite gneiss that differs from the leucogneiss mainly for higher biotite and lower microcline contents. This mesocratic gneiss presents granonematoblastic texture and is fine-grained. It is composed of quartz (13-20%), plagioclase (33-39%), biotite (20-27%), microcline (2-7%), titanite (5-10%), hornblende (1-10%) and, as accessories, may contain metamorphic clinopyroxene, zircon, apatite and opaque minerals (Figure 4). Modal analyses (Figure 5) allowed attributing to this lithotype a tonalitic composition.

These gneisses are frequently interlayered or associated to a metasedimentary sequence, characterized by heterogeneous paragneisses (Figure 6) that can be described as a succession, in varied scales, of different types of biotite-muscovite-garnet-sillimanite gneiss, locally with centimetric to metric bands or lenses of quartzites, gondites and

cherts. Within the NE-SW shear zones, these rocks display overall migmatitic textures (Figure 7) and muscovite is not present.

The metabasic rocks of the Oliveira Fortes Unit show composition ranging from quartz dioritic/gabbroic to dioritic/gabbroic, and occur as centimetric to hectometric tabular bodies, invariably parallel to the structures of the country supracrustal sequence rocks described above (Figure 2). Based on detailed petrographic analyses, and following an order from the least the most deformed rocks, it is possible to individualize four main lithotypes for the metabasic rocks unit: metagabbro, garnet metagabbro, (garnet) amphibolite and biotite amphibolite.

The two types of metagabbro (metagabbro and garnet metagabbro) are fine to medium and locally coarse-grained with subophtic and granular texture
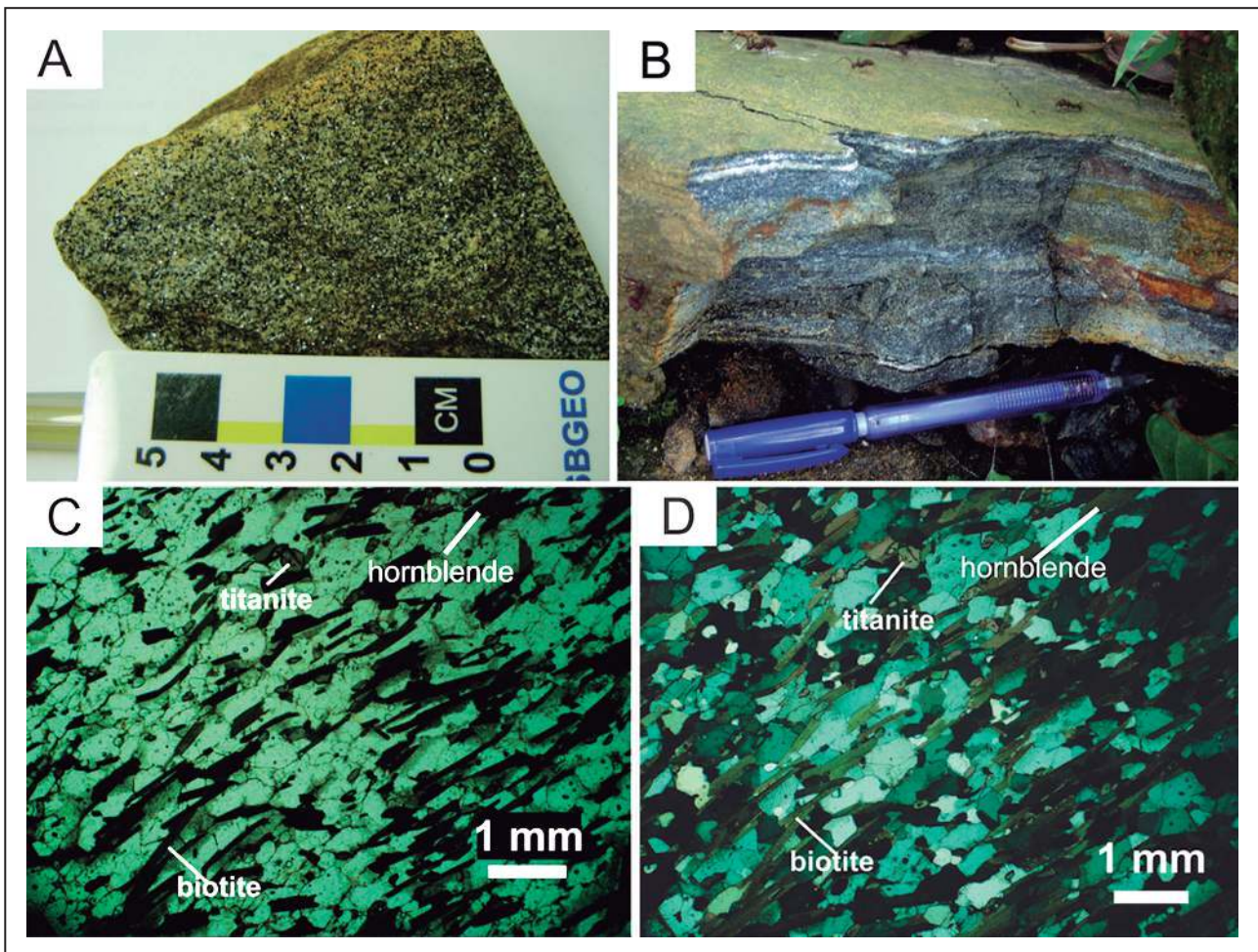

Figure 4 Aspects of the (hornblende)-biotite gneiss; A. hand sample with mesocratic and homogeneous aspect; B. outcrop view; C-D. granonematoblastic texture with titanite and oriented hornblende and biotite crystals under parallel nicols and crossed polars.
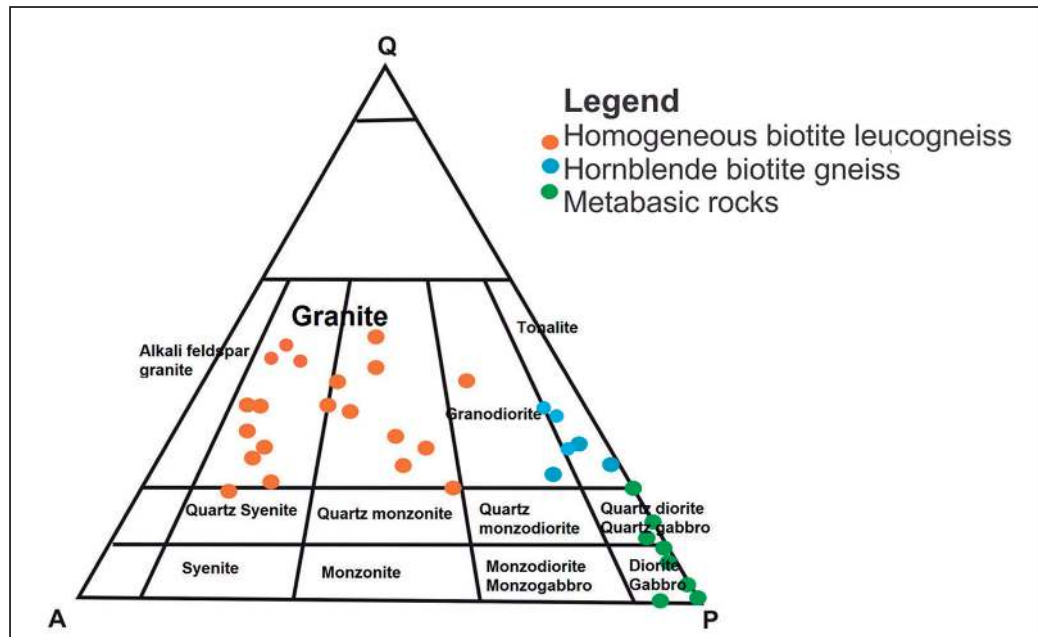
Figure 5 Compositional QAP (Q- quartz, A- alkali feldspar, P- plagioclase) diagram (Streickeisen, 1976) for metabasic rocks (green plots), homogeneous biotite leucogneiss and (hornblende)-titanite-biotite gneiss.
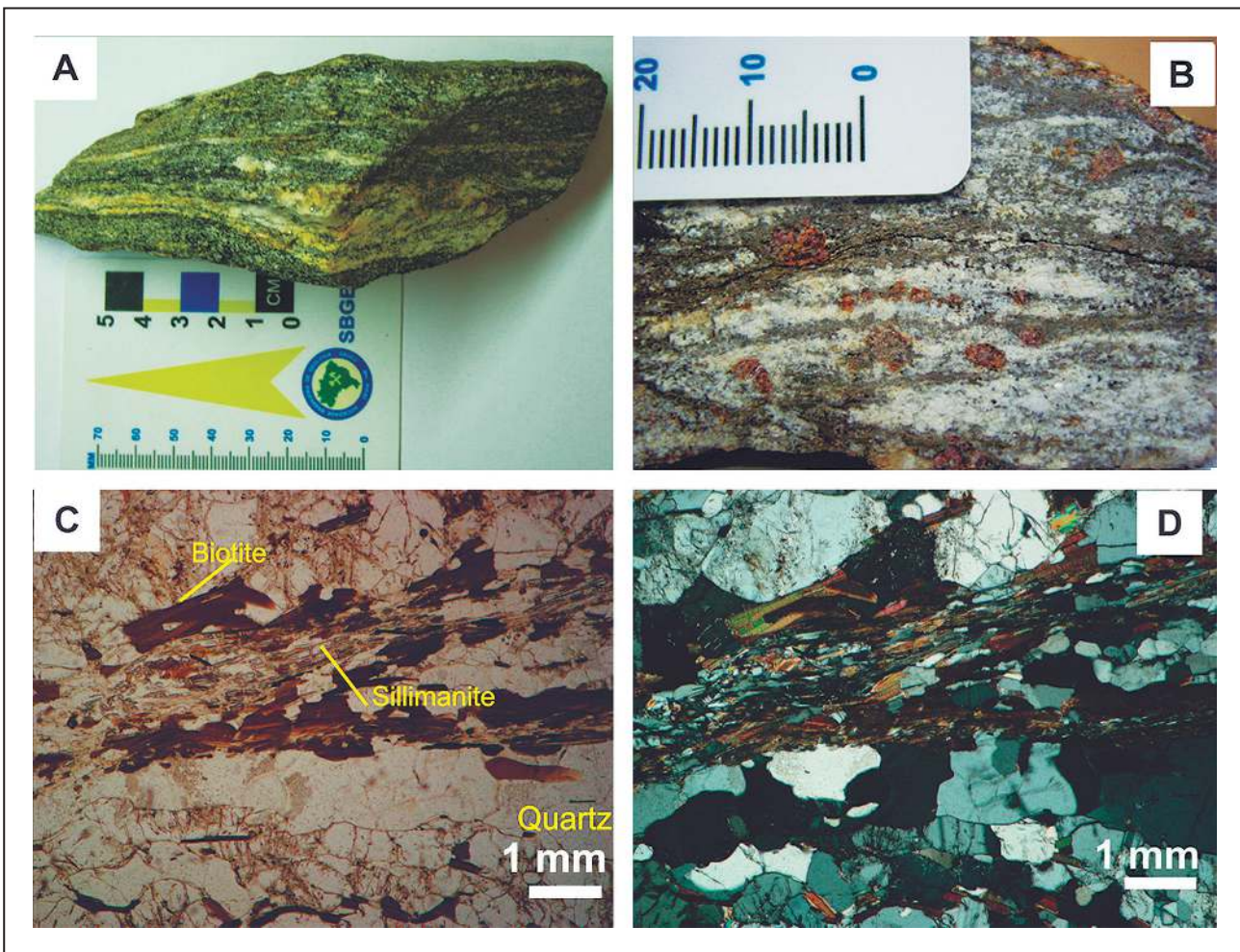

Figure 6 Aspects of the heterogeneous biotite gneiss; A. gneiss banding with leucocratic and mesocratic bands; B. sillimanite-garnet-muscovite-biotite gneiss with garnet porfiroblasts; C-D. garnet-muscovite-biotite gneiss exhibiting well developed crystals of sillimanite under parallel nicols and cross nicols.
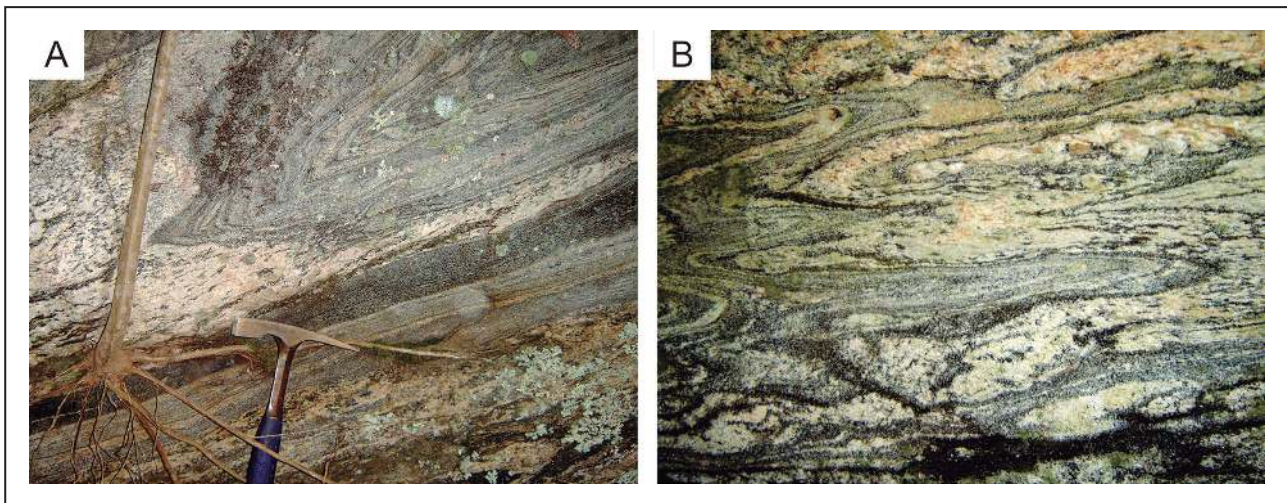
Figure 7 Aspects of the (sillimanite)-garnet-biotite gneiss; A. migmatitic texture; B. schilieren structure.

(Figure 8A, C-D), mainly composed of metamorphic clinopyroxene (probably augite), and plagioclase (labradrorite), and varied contents of orthopyroxene (hypersthene), also metamorphic hornblende, garnet, magnetite and ilmenite. Based on pethrographic analisys and their disequilibrium textures, it is assumed that the two types of metagabbros, have a metamorphic clinopyroxene and hornblende grains, on the other hand the orthopyroxene grains probably are relicts of the previous igneous phase, since no reaction to generate this last mineral could be observed in thin section. The first litothype is medium to coarse grained and its mineralogy is formed by orthopyroxene, clinopyroxene, plagioclase and magnetite, hornblende occurring as a subordinate phase. Despite being texturally very similar to the metagabbro, the garnet metagabbro contains coronas of garnet and magnetite around plagioclase, hornblende, and clinopyroxene (Figure 8E-F). The (garnet) amphibolite is a medium to fine-grained rock and displays granonematoblastic to mylonitic texture (Figure 8G-H). The mineralogical assembly is composed essentially of hornblende, plagioclase, titanite and garnet. Igneous orthopyroxene is absent and metamorphic clinopyroxene may appear also as relict minerals.

The biotite amphibolite is fine-to medium-grained, displaying inequigranular granoblastic to nematoblastic array (Figure 8I-J), with protomylonitic texture and local mineral stretching (Figure 8B). The paragenesis is composed essentially of hornblende, plagioclase and biotite with titanite, apatite, clinopyroxene, quartz and opaque minerals as accessories. This unit is observed in the higher deformation areas, therefore the constituient minerals are constantly deformed and recrystallized. Moreover, in these areas, the hornblende crystals are altering to biotite, and titanite reaches to compose 4% of rock.

The metabasic rocks display a highly varied structures pattern, since magmatic preserved subo-phitic textures, with massive aspect, to mylonitic structures, with stretched minerals, closely associated with NE-SW shear zones, where the biotite amphibolite predominate.

Near the thrust boundary (Figure 1), NE-SW low angle ductile shear zones are associated to open to isoclinal folding, and a mylonitic foliation is frequent, and can be characterized in outcrops by a constant compositional banding, giving a strong intercalation between mesocratic and leucocratic layers. Locally, there are rotated feldspar porphyroclasts, L-tectonites and quartz ribbons. In thin section, this pattern is characterized by the presence of quartz ribbons in a fine-grained recrystallized matrix, which displays a protomylonitic texture. At less deformed areas structures as irregular compositional banding and/or penetrative schistosity occur, showing, in thin section, a granoblastic texture and few or almost no evidence of dynamic recrystallization.

In the areas where deformation is less intense, pelitic rocks bear primary muscovite and show no longer evidences of partial melting. These indicate a medium-grade metamorphism under
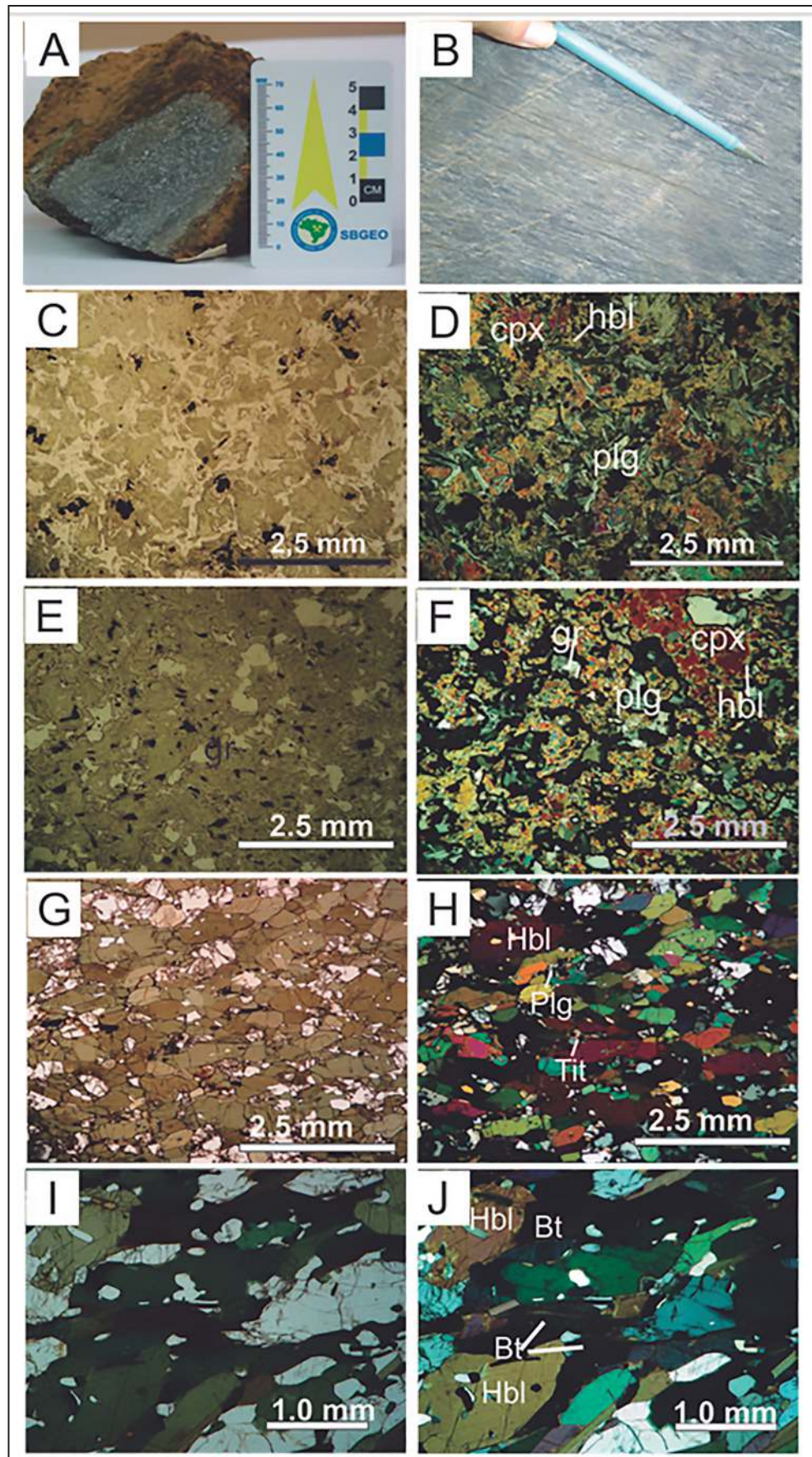
Figure 8 Aspects of the metabasic rock of Oliveira Fortes unit; A. metagabbro hand sample; B. Strongly deformed amphibolite showing penetrative foliation; C-D. Metagabbro showing preserved subophitic texture under parallel nicols and crossed pollars; E. Garnet metaggabro showing coronas of garnet around grains of plagioclase slightly recrystallized; F. same as "E" under crossed pollars (x 2.5).; G-H. Amphibolite with nematoblastic texture under parallel nicols and crossed pollars; I and J. Biotite amphibolite exhibiting biotite in the borders of hornblende grains under parallel nicols and crossed pollars.

lower amphibolite facies conditions. On the other hand, in the most deformed areas, under influence of shear zones, evidences of medium to high-grade metamorphism are revealed by the presence of schlieren and stromatic migmatitic textures, well developed within pelitic rocks, indicating that conditions of partial melting were overcome. The presence of sillimanite and anatetic leucosome with granitic composition, added to the absence of primary muscovite, point to metamorphism under upper amphibolite facies condition.

4 Lithogeochemistry

The analysed rocks (Table 1) correspond to eight samples of metabasic rocks of Oliveira Fortes (metagabbros and garnet amphibolites), four samples of homogeneous biotite leucogneiss and one sample of hornblende-biotite gneiss. As the area is affected by tectonism that developed several shear zones, which are often related to metassomatic processes, care was taken to avoid sampling within these zones. Thus, with the exception of sample EF-24, which was sampled near to, but not within, the thrust zone, sampling was carried out far away from this and all other minor shear zone areas. Moreover, sample selection was performed on the basis of petrographic analyses in order to preclude post-magmatic chemical modification processes. Thus, all selected metabasic rocks bear no biotite, no quartz and show subophitic or granoblastic texture; none of them presents mylonitic texture (Table 2).

4.1 Metabasites

The metabasites of Oliveira Fortes unit plot in the field of gabbro, show a subalkaline nature (Figure 9A), with tholeiitic affinity (Figure 9B).

From the binary diagrams, it can be observed that the majority of the oxides display a negative correlation with MgO, except CaO and Al_2O_3 (Figure 10).

Continuing the analysis of binary diagrams, were chosen for composition projections, trace elements with the following characteristics: two compatible elements (V and Co); one immobile incompatible element (Zr); and one mobile incompatible element (Ba). With the exception of

Co and Ba the other trace elements display a clear negative correlation with MgO (Figure 10).

With regard to the method of minimal squares, it is known that to be considered a meaningful correlation result, the values of the squares of the Pearson's correlation coefficients must be within the 95 - 99% interval. For the majority of the oxides/ elements of the studied metabasites yield poor results (Table 3): values are below 80% for Al_2O_3, CaO, Fe_2O_3, MnO and all the trace elements with the exception of V which yields good values within the 95-99% interval.

This suggests that the set of basic samples cannot be related by a process of fractional crystallization and, therefore, it is most probable that all the samples do not belong to the same suite. A hypothesis that can be brought up is that the samples could be correlated by processes of partial melting, and may be associated to different quantities of partial melting from a same source, or been generated by partial melting of different sources. To test these hypothesis rare earth elements geochemical modeling will be discussed in a following section.

Incompatible elements ratios do not vary substantially during fractional crystallization processes and thus it is expected a maximum variation of 1.5 times among cogenetic rocks (Cox *et al.* 1979). Some authors such as Cullers *et al.* (1974) and Muecke *et al.* (1979) indicate that there is usually little modification of the rare earth elements during the metamorphic events and, therefore, we can use them for the geochemical analysis of the protolith. For this reason, $[La/Yb]_N$ ratios were applied in order to verify any relation between samples (Table 1).

In an attempt to relate values of MgO with $[La/Yb]_N$ ratios, it was verified that the increase of MgO do not correspond to the increase or decrease of $[La/Yb]_N$. This fact corroborates with the fact that the analyzed samples cannot be part of only one suite, meaning that they are not all cogenetic.

4.1.1 Geochemistry of the Rare Earth Elements and Multi-Element Diagrams

On the basis of $[La/Yb]_N$ ratio values (Table 1), samples were subdivided into three groups. In the first group, metabasites display lower values

Sample	EF-24	EF-52	EF-65A	EF-66	EF-69	EF-91	EF-92	DAT-44	EF-10	EF-68B	EF-93	DAT-84	DAT-124
Rock	met	met	met	met	met	met	Met	met	bt-leu	bt-leu	bt-leu	bt-leu	hb-bt-gn
SiO_2	47.7	46.03	48.33	49.29	48.69	49.21	47.71	48.65	70.6	71.41	75.35	67.37	71.21
TiO_2	2.39	2.48	1.78	2.37	1.66	1.47	3.46	1.59	0.27	0.35	0.12	0.46	0.30
Al_2O_3	13.93	14.00	14.49	14.07	14.68	12.63	13.39	14.73	14.78	13.93	13.52	16.18	15.20
Fe_2O_3	12.91	15.00	12.11	13.80	12.67	16.27	15.47	12.15	2.74	2.77	1.18	3.87	1.92
MnO	0.18	0.21	0.18	0.21	0.19	0.22	0.20	0.18	0.03	0.03	0.02	0.04	0.02
MgO	6.88	6.37	7.09	6.02	7.26	5.59	5.23	7.45	0.75	1.02	0.27	1.36	0.68
CaO	11.00	9.46	10.82	9.81	10.65	9.65	8.78	11.02	2.37	1.97	1.10	3.76	2.02
Na_2O	2.29	1.79	2.20	2.35	2.26	2.40	2.74	2.19	3.76	2.58	2.98	4.10	3.40
K_2O	0.56	0.54	0.55	0.67	0.53	0.45	0.90	0.49	3.09	5.12	4.53	1.66	3.48
P_2O_5	0.23	0.24	0.22	0.25	0.19	0.14	0.53	0.18	0.13	0.16	0.05	0.28	0.10
LOI	0.91	2.62	1.21	0.36	0.75	1.22	0.40	0.86	1.45	0.67	1.10	0.87	1.82
Total	98.98	98.74	98.98	99.20	99.53	99.25	98.81	99.49	99.97	100.01	100.22	99.95	100.15
V	333	382	315	387	310	348	394	281	29	42	12	63	25
Ba	141	153	154	184	143	70	402	167	676	2193	905	634	1346
Sr	329	182	258	225	223	118	482	406	283	457	213	889	311
Y	21	31	23	41	23	28	32	19	8	8	15	10	7
Zr	109	152	109	141	101	87	236	90	162	184	178	107	157
Co	48	53	53	46	61	82	57	64	19	26	11	14	11
Rb	16	18	16	31	13	7	27	10	121	162	115	76	90
Nb	15	18	12	14	12	6	33	14	8	8	3	4	4
La	15.7	23.9	18.3	32.8	15.1	13.7	56.9	18.6	25.9	40.2	83.8	44.5	64.9
Ce	36.1	49.7	38.6	37.6	33.2	22.2	111	40.1	86.4	121	172	90.7	61.5
Pr	4.62	6.48	4.67	7.39	4.17	3.5	13.2	4.99	5.13	8.2	15.3	10.2	10.2
Nd	20.2	27.2	19.3	30.1	17.9	15.8	53.7	20.7	16.7	26.6	50.2	36.2	33.3
Sm	4.9	6.4	4.4	6.8	4.3	4	10.2	4.5	2.9	4.3	7.7	5.5	4.4
Eu	1.99	2.39	1.7	2.43	1.61	1.46	3.44	1.69	0.67	1.53	1.44	1.43	1.87
Gd	4.8	6.4	4.6	7	4.3	4.3	8.6	4.1	2	2.5	4.4	3.4	3.3
Tb	0.8	1.1	0.8	1.2	0.8	0.8	1.3	0.7	0.3	0.4	0.6	0.4	0.3
Dy	4.7	6.6	4.8	7.4	4.8	5.3	6.9	3.8	1.8	1.8	3.1	2.2	1.5
Ho	0.9	1.3	0.9	1.4	0.9	1.1	1.2	0.7	0.3	0.3	0.6	0.4	0.2
Er	2.3	3.5	2.5	4	2.6	3	3.4	2	0.9	0.8	1.8	1	0.7
Tm	0.32	0.5	0.37	0.56	0.38	0.46	0.47	0.28	0.13	0.1	0.27	0.14	< 0.05
Yb	1.9	3.2	2.3	3.5	2.4	2.9	2.8	1.7	0.8	0.6	1.8	0.8	0.5
Lu	0.27	0.46	0.34	0.51	0.37	0.45	0.39	0.25	0.11	0.08	0.28	0.11	0.07
Hf	3.1	4.2	3	3.9	2.8	2.5	6.2	2.7	4.3	4.7	5.2	2.8	4
Ta	1.1	1.3	0.9	1.1	0.9	0.7	2.5	1.1	0.7	0.6	0.3	0.6	0.2
Th	1.7	2	1.8	1.7	1.2	0.6	3.4	1.6	17.8	15	66.7	5	4.5
Total REE	99.5	139.13	103.58	142.69	92.83	78.97	273.5	104.11	144.04	208.41	343.29	196.98	182.74
Eu/Eu*	1.25	1.13	1.15	1.07	1.14	1.07	1.12	1.20	0.85	1.42	0.75	1.00	1.49
[La/Yb]N	5.59	5.05	5.38	6.35	4.25	3.19	13.74	7.4	21.87	45.5	31.47	37.56	87.96

Table 1 Whole-rock, major and trace element geochemistry for metabasic rocks (met), biotite leucogneiss (bt-leu) and (hornblende)-biotite gneiss (hb-bt-gn).

Samples	Lithotype	Plg	Hbl	Cpx	Opx	Gr	Op	Tit	Qtz	K-f	Bt	Musc	Ap	Zr
EF-24	Titanite amphibolite	45	38	8		1.5	2.5	9						
EF-52	Titanite amphibolite	44	32	11		4	4	5						
EF-65	(Titanite)-garnet metagabbro	35	39	12		6	6	2						
EF-66A	Garnet amphibolite	40	37	8		12	3							
EF-69	Garnet - titanite amphibolite	32	38	7		11	6	6						
EF-91	Garnet - titanite amphibolite	29	37	26			3	5						
EF-92	Garnet metagabbro	31	36	7	12	8	6							
DAT-44	Garnet metagabbro	40	28	32		11.2	2.8							
EF-10	Biotite leucogneiss	18					1		33	29	16	2		1
EF-68B	Biotite leucogneiss	11.5					1	1.2	28	39	11.5	0.5		0.5
EF-93	Biotite leucogneiss	13.2					2		34	32	14	1		2.4
DAT-84	Hornblende-biotite leucogneiss	38	6				1	5	16	6	25		1.5	2.5
DAT-124	Biotite leucogneiss	20					1		32	29.5	15	1.5		1

Table 2 Mineralogical composition of metabasic rocks of Oliveira Fortes unit and gneisses of Conceição do Formoso group used in geochemical analysis.
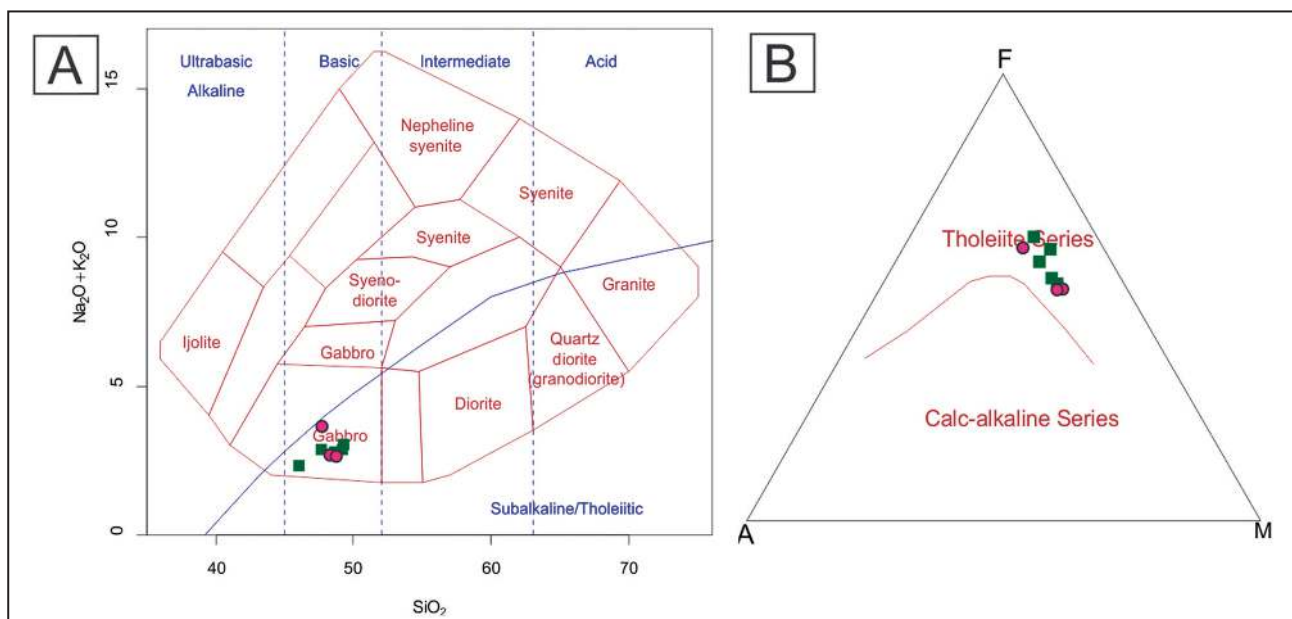

Figure 9 Chemical classification for the metabasite rocks of Oliveira Fortes unit; A. TAS diagram (Total alkalis x SiO$_2$) of Cox *et al.* (1979); B. AFM (A- Na2O + K2O; F- FeO+ 0.9 Fe2O3= FeT; M- MgO) diagram of Irvine & Baragar (1971) (right). Dark green symbols: amphibolites; pink symbols: metagabbros.

of [La/Yb]$_N$ (3.19 and 4.25) and, therefore, lower fractionation of the elements is observed. The second group, that yields [La/Yb]$_N$ values between 5.00 and 7.40, displays a higher fractionation of the light rare earth elements. The last group consists only of one sample (EF-92) and shows light rare earth elements enrichment, displaying, consequently, a highly fractionated pattern ([La/Yb]$_N$ - 13.74).

A small positive anomaly of Eu (Table 1) is observed in all samples and could be attributed to accumulation of plagioclase during differentiation of mafic, underplated magmas (Rudnick et al., 1986; Kempton et al., 1990) (Figure 11).

To illustrate the geotectonic environment in the formation of the metabasic rocks, were used binary or ternary diagrams of Pearce & Norry (1979)
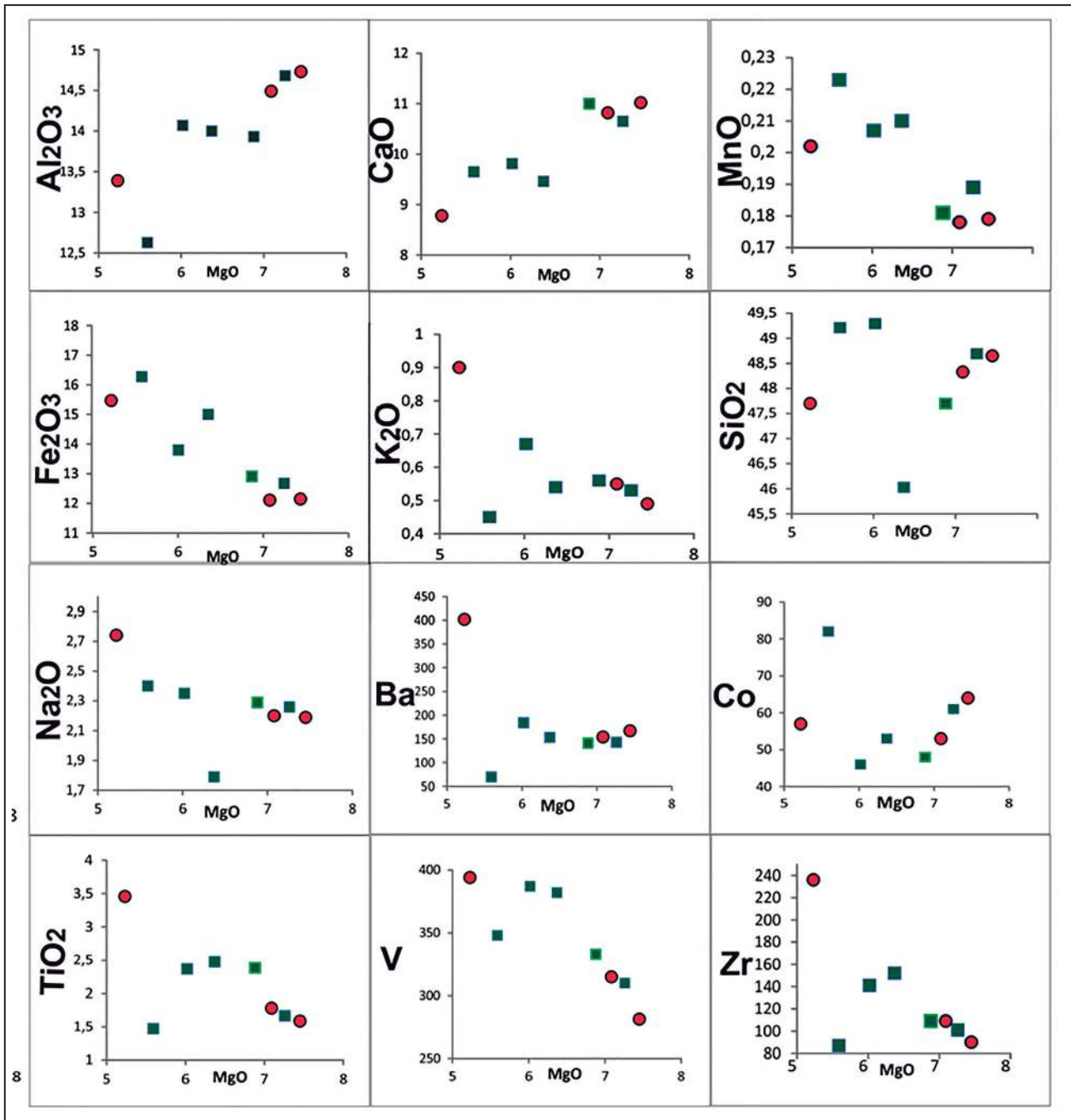
Figure 10 MgO versus major and trace element for metabasic rocks of Oliveira Fortes unit. Dark green symbols: amphibolites; pink symbols: metagabbros.

(Figure 12A), Pearce & Cann (1973) (Figure 12B) and Meschede (1986) (Figure 12C) that indicate a predominantly intraplate environment.

In order to identify the genesis and the geotectonic environment in which these rocks were generated, it was made the chondrite-normalized $[La/Yb]_N$ and $[La/Nb]_N$ ratios (Thompson, 1982). Based on the obtained values it can be observed

that the rocks of Oliveira Fortes unit were generated from a process of melting of the enriched mantle, suggesting the subcontinental lithospheric mantle as source material and pointing to a geotectonic environment like that of the intraplate flood basalt provinces. In addition, chondrite-normalized multi-element diagrams (Thompson, 1982) were generated in order to establish a comparison with chondrite normalized diagrams for basic rocks and

Element	(R2)L	NSL	(R2)P	NSP
Al_2O_3	0.7353	95-99%	0.7378	95-99%
CaO	0.8379	99-99.9%	0.8385	99-99.9%
Fe_2O_3	0.8198	95-99%	0.8252	95-99%
K_2O	0.3433	<80%	0.4384	<80%
MnO	0.6474	90-95%	0.7208	95-99%
Na_2O	0.2881	<80%	0.6421	90-95%
SiO_2	0.0006	<80%	0.0756	<80%
TiO_2	0.3461	<80%	0.3485	<80%
Ba	0.2059	<80%	0.472	<80%
Co	0.03	<80%	0.214	<80%
V	0.7197	95-99%	0.8441	99-99.9%
Zr	0.4289	<80%	0.4693	<80%

Table 3 Values of the squares of the Pearson's correlation coefficients ((R2)L and (R2)P), where (R2)L = linear correlation coefficient and (R2)P = polynomial correlation coefficient and associated meaningful levels (NSL e NSP).

suites of modern environments. The result (Figure 13) indicates a great resemblance to the intraplate basalts of Decan and Paraná, pointing again to the hypothesis that the protoliths of these rocks were originated from continental basaltic floods.

Lastly, considering that these metabasites are not correlated by a process like fractional crystallization, it was carried out a partial melting geochemical modeling as proposed by Pearce (1968). Partial melting geochemical modeling was performed on the basis of the obtained $[La/Yb]_N$ ratio values (Table 1). Results of geochemical modelling indicate that different rock generating magmas could not have been generated from the same source. Having as base the

partial melting experiments of Mysen and Kushiro (1977), performed in peridotite nodules, and the experiments of Walter and Presnall (1994), carried out in lherzolite of simple composition, *Ne*-free melts form by a minimum of 25% partial melting. Furthermore, 45% would be the expected maxima limit of degree of partial melting; above this value, melts generated would be komatiitic. However, the performed geochemical modelling yields some unexpected results: it would be necessarily a higher than 45% degree of melting to generate the 3.20 $[La/Yb]_N$ ratio value of one of the metabasic samples; and it would be necessarily degrees lower than 25% of partial melting to generate $[La/Yb]_N$ ratio of 13.7. Thus, different amounts of partial melting from the same source could be discarded. In this way, the more plausible scenario is that the protoliths of the study metabasic rocks were generated by partial melting of different mantle sources. A very heterogeneous subcontinental lithospheric mantle should be considered as the local source.

4.2 Gneisses of Conceição do Formoso Group

Four samples of homogeneous biotite leucogneiss and one sample of (hornblende)-biotite gneiss were analyzed (Table 1). The geochemical data show SiO_2 contents between 70.60 and 75.35, for the biotite leucogneisses, indicating a rhyolitic composition, and between 63.9 and 67.37, for the hornblende-biotite gneisse, pointing to a dacitic composition (Figure 14 A). All five samples belong to the calc-alkaline series (Figure 14 B) and display weak peraluminous character (A/CNK > 1) (Figure 14 C).
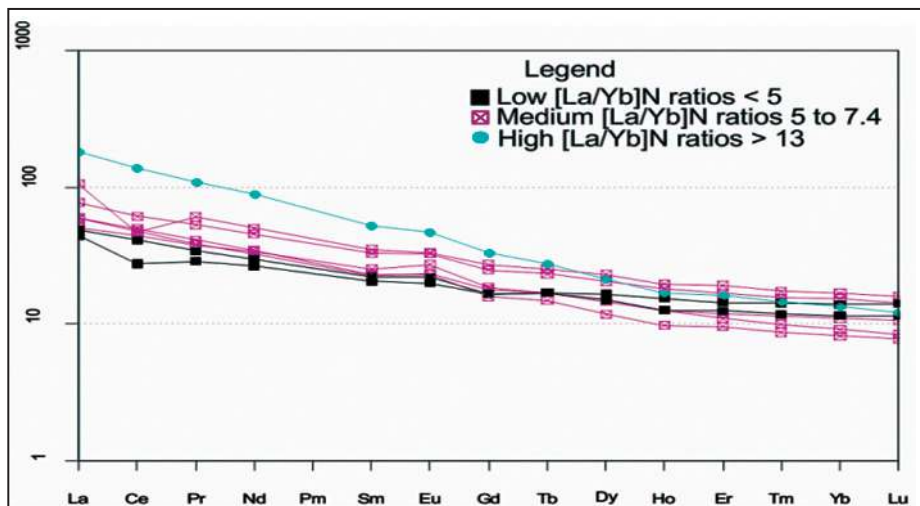

Figure 11 Chondrite normalized rare earth elements pattern (Boynton, 1984) of Oliveira Fortes unit. The first group (black squares) has low $[La/Yb]_N$ ratio values ranging from 3.19 to 4.25. In the second group (pink squares) $[La/Yb]_N$ ratio varying from 5.0 to 7.4. In the last group (blue circles) with a single sample presents $[La/Yb]_N$ ratio = 13.74.
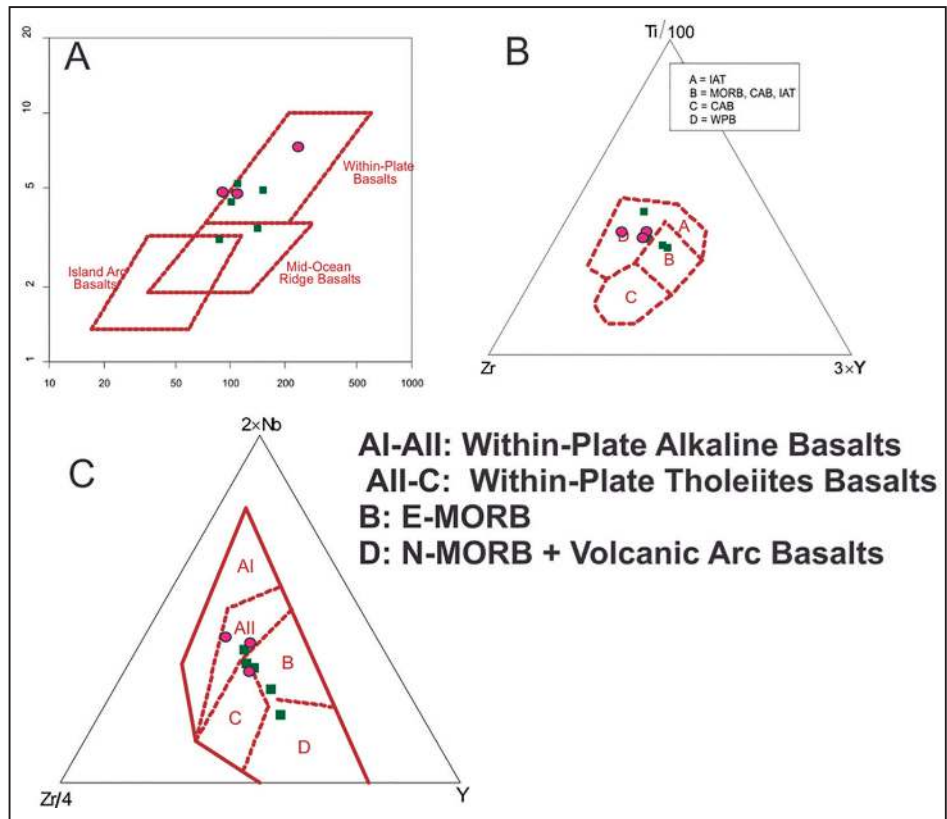
Figure 12 Tectonic setting diagrams for the metabasic rocks of Oliveira Fortes unit; A. Pearce & Norry (1979); B. Pearce & Cann (1973); C. Meschede (1986). Dark green symbols: amphibolites; pink symbols: metagabbros.
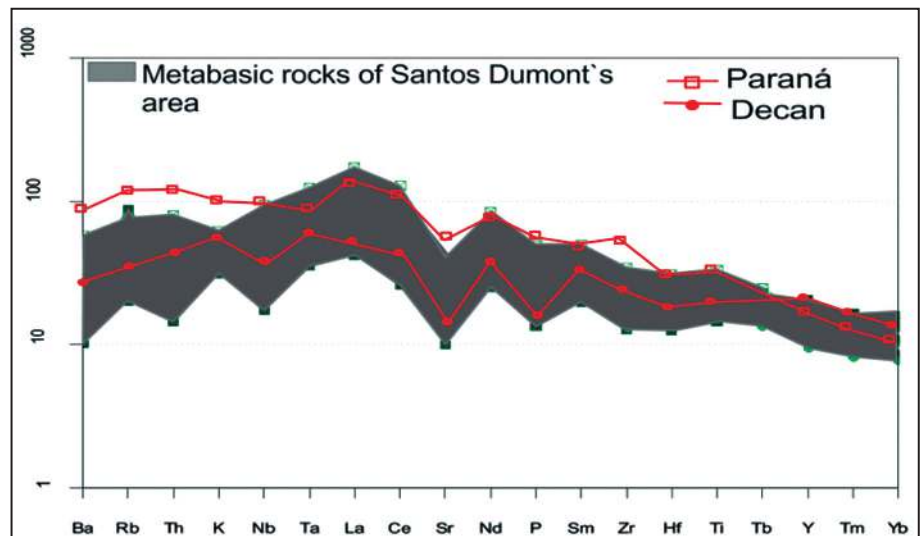

Figure 13 Chondrite-normalized multi-element diagrams for the metabasites of Oliveira Fortes unit. Emphasis on the simillarity with the Decan and Parana's signature (red line).

4.2.1 Geochemistry of the Rare Earth Elements and Spidergrams

Gneisses of Conceição do Formoso Group show rare earth elements patterns of light REE enrichment (Figure 15A) and, at least, two groups can be separated, based on Eu anomalies; the first group presents a positive anomaly (Eu/Eu* ~ 1.4); the other group composed of two samples shows a negative anomaly (Eu/Eu*~0.8).

4.2.2 Geotectonic Environment

Gneisses of Conceição do Formoso Group (Figure 15B) display enrichment in mobile elements (Ba, Rb, Th, K) and negative anomalies of Nb, Sr and P, which are typical signatures of destructive margin environments (volcanic arcs).

Negative anomalies were observed for P and Sr which can be controlled by apatite and plagioclase
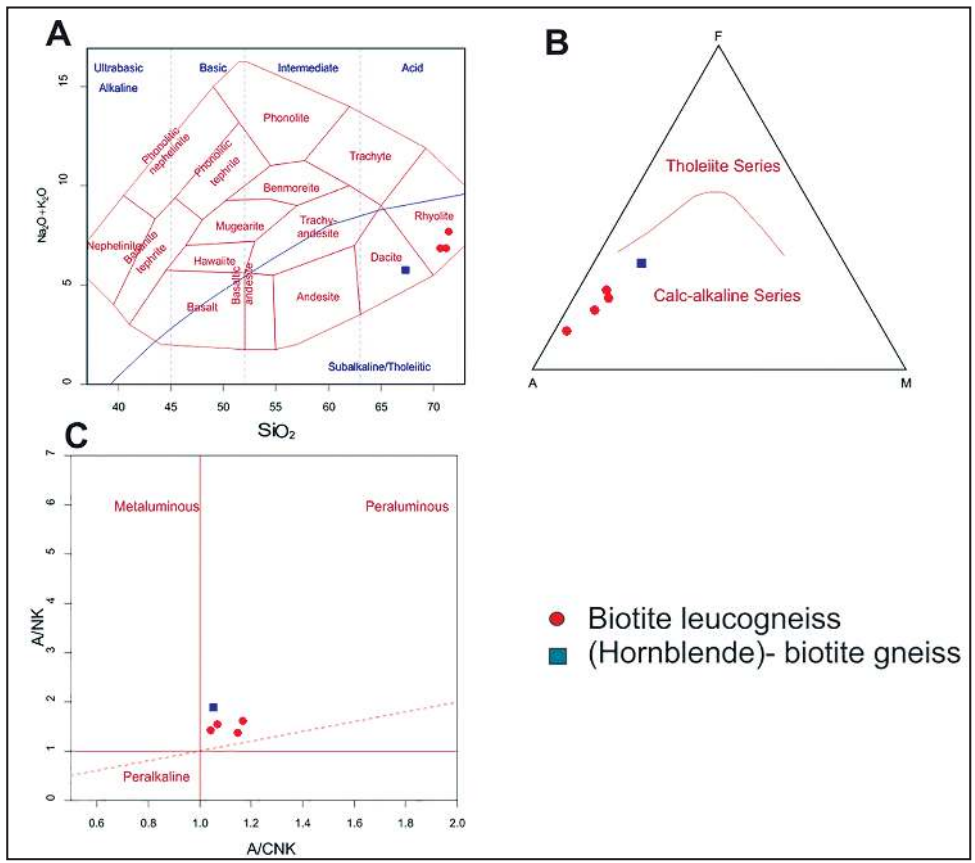
Figure 14 Chemical classification diagrams for the gneisses of Conceição do Formoso Group; A. TAS diagram of Cox *et al.* (1979); B. AFM diagram of Irvine & Baragar (1971); C. A/NK x A/CNK diagram of Maniar & Piccoli (1989) based in Shand's index. Red symbols: biotite leucogneiss; blue symbols: (hornblende)-biotite gneiss.
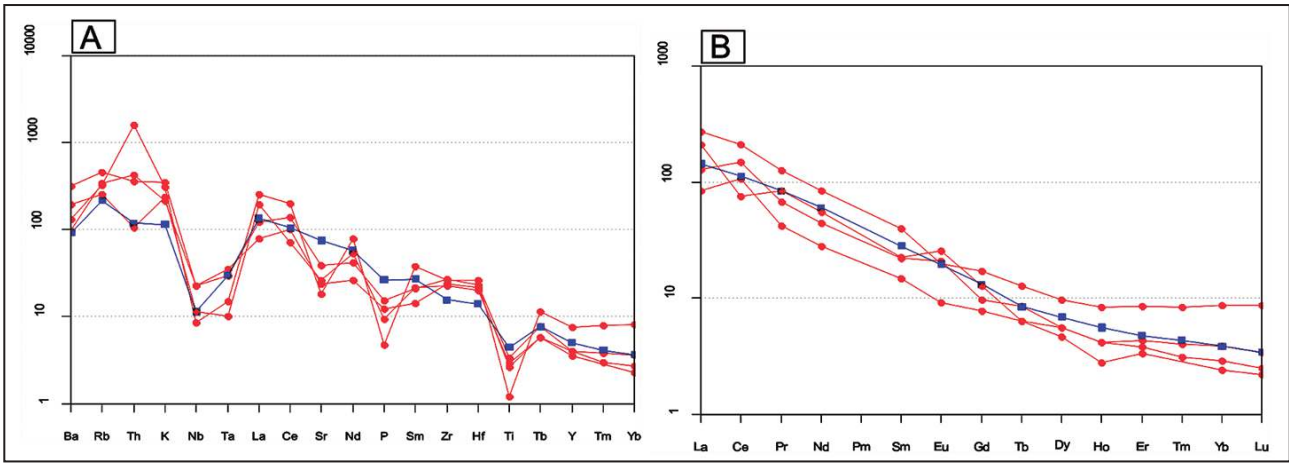

Figure 15 – A. Chondrite normalized rare earth element pattern of gneisses of Conceição do Formoso Group.; B. chondrite-normalized multi-element diagrams of gneisses of Conceição do Formoso Group. Red symbols: biotite leucogneiss; blue symbols: (hornblende)-biotite gneiss.

fractionation. Nb is controlled by ilmenite, rutile and titanite fractionation. The metavolcanic rocks were probably generated in a subduction environment (volcanic arc) as can be observed in the Rb/Y+Nb *x* Nb/Y diagram (Pearce *et al.,* 1984) (Figure 16).

5 Geological and Lithogeochemical Conclusions

The NE-SW shear zones are characterized by SE low angle stretching lineation, near down-

dip and are associated to tight to isoclinals folds. These structures points to a strong correlation with deformation phases attributed to the structural evolution of the Ribeira belt (Nogueira 1999; Nogueira et al. 2003). The low angle shear zones affected the rocks that had already been through a previous history of deformation, causing migmatization and formation of protomylonitic textures. Within the less deformed areas, structures associated with the older deformation are preserved
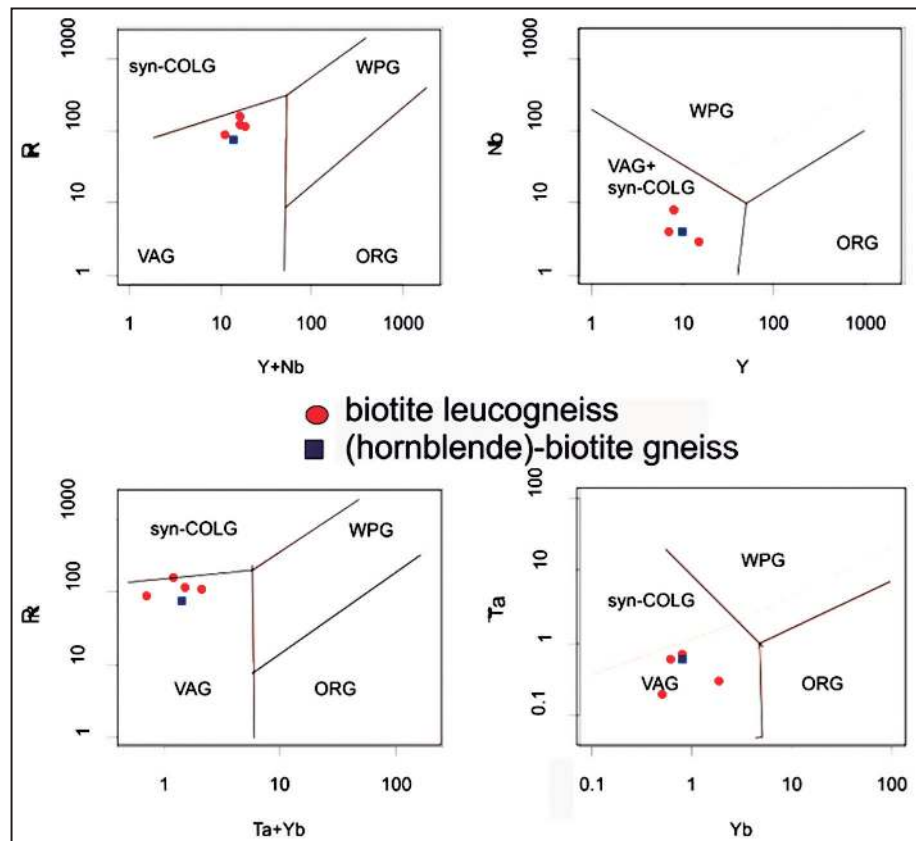
Figure 16 Tectonic diagram of Pearce *et al.* (1984) for the gneisses of Conceição do Formoso Group Red symbols: biotite leucogneiss; blue symbols: hornblende biotite gneiss.

and display open folds with low angle NE and SW limbs, related to the Araçuaí belt structures. The metamorphic minerals content indicates that in this region the rocks were metamorphosed under lower to upper amphibolite facies conditions.

Geochemical studies indicate that the metabasites characterize a subalkaline series, with tholeiitic affinity and gabbroic composition. Based on quantitative statistical analysis, made with the purpose of verifying cogeneticity among the study rocks, it was observed that the basaltic magmas were generated from melting of a mantle source with, at least, a contribution of the subcontinental lithospheric mantle. Geochemical data, which attest the absence of cogeneticity among the study metabasites, indicate that local subcontinental lithospheric mantle source was heterogeneous and, thus, capable of generate the magmas that gave origin to the study metabasites. According to the obtained results, it can be affirmed that these magmas were continental basalts, hosted in the form of dikes or sill in an intraplate environment.

For the gneisses of Conceição do Formoso Group, features such as fine homogeneous texture and the presence of preserved euhedral phenocrysts of microcline suggest a volcanic origin. In terms of its chemical composition, they constitute a calc-alkaline series with weak peraluminous character and their protoliths have riolitic and dacitic compositions. Negative anomalies for P, Sr, Nb e Ti suggest the participation of apatite, plagioclase, ilmenite and titanite as fractionate minerals during magmatic differentiation. These rocks have geochemical signature of arc environment, possibly involving processes of crustal contamination. Together with the paragneisses, these gneisses form a possible volcanossedimentary sequence, which are considered as country rock to the metabasic rocks.

6 Final Remarks: Regional Correlations

According to Brandalise *et al.* (1991b), the Mantiqueira Complex comprises tonalitic/trondhjemitic and granitic/granodioritic banded gneisses with tabular intercalations of metabasites. This unit corresponds to the arquean-paleoproterozoic basement, which crops out from the northernmost portion of the Araçuaí Belt to the southern portion, in the region of Lima Duarte to the west of Juiz de

Fora (Pedrosa Soares *et al.*, 2001). The lithotypes of the Santos Dumont region have been interpreted as belonging to the Mantiqueira Complex (Brandalise *et al.*, 1991a, 1991b; Silva *et al.*, 2002; Peres *et al.*, 2004; Alkmim *et al.*, 2007), however, according to the data presented here, in the north of the thrust boundary of Santos Dumont region (Figure 1), these rock associations were not found.

Some authors also include these rocks within the Piedade Gneiss or Complex (Ebert, 1958; Machado Filho *et al.*, 1983; Silva *et al.*, 2002). However, Hasui & Oliveira (1984) also associated the Piedade Gneiss with ultrabasic, granitic to tonalitic rocks, which were not observed in the area.

For these reasons, the name Conceição do Formoso Group is proposed for the characterization of the metavolcanossedimentary sequence in order to dissociate this unit from these two regional units (Mantiqueira Complex and Piedade Gneiss or Complex).

The Conceição do Formoso Group consists of a supracrustal sequence composed of biotite leucogneiss, possibly of volcanic origin, interlayered with biotite paragneiss. This unit might be partially correlated to the Tiradentes suite, a subvolcanic-volcanic unit composed of dacites, granophyres, mafic andesites and intrusive tonalites, whose felsic rocks present some preserved igneous features such as microporphyritic and porphyritic textures with subhedral phenocrysts of plagioclase in a granophyric matrix (Ávila *et al.*, 2014).

This sequence has also similarities with the rocks of the Dom Silvério Group, defined by Brandalise (1991a), which comprehends, in general, a metavolcanossedimentary assembly that includes pelitic schists, amphibolites, quartzites and, subordinately, gondites, metaultramafic rocks and iron formations. This correlation requires geological mapping and more detailed information about the area between these regions, in order to bring subsides for this discussion.

7 Acknowledgements

8 References

Almeida, F.F.M.; Hasui, Y.; Brito-Neves, B.B & Fuck, R.A. 1977. As províncias estruturais do Brasil. *In*: SIMPÓSIO DE GEOLOGIA DO NORDESTE, 8, Campina Grande, 1977, *Atas do VIII Simpósio de Geologia do Nordeste*, Campina Grande, SBG, p. 363-391.

Almeida, F.F.M.; Hasui, Y.; Brito-Neves, B.B & Fuck, R.A. 1981. Brazilian Structural Provinces: an introduction. *Earth-Science Reviews*, *17*: 1-29.

Ávila, C.A.; Teixeira, W.; Bongiolo, E.M.; Dussin, I.A. & Vieira, T.A.T. 2014. Rhyacian evolution of subvolcanic and metasedimentary rocks of the southern segment of the Mineiro belt, São Francisco Craton, Brazil. *Precambrian Research*, *243*: 221-251.

Brandalise L.A. 1991a. Programa de Levantamentos Geológicos Básicos do Brasil. Folha Ponte Nova, SF.23-X-B-II. Escala 1:100.000. Brasília, DNPM/CPRM, 194p.

Brandalise L.A. 1991b. Programa de Levantamentos Geológicos Básicos do Brasil. Folha Barbacena, SF.23-X-C-III. Escala 1:100.000. Brasília, DNPM/CPRM, 194p.

Boyntom,W.R. 1984. Cosmochemistry of the rare earth elements meteorite studies. In HENDERSON, P. (ed), Rare Earth Element Geochemistry. Amsterdan, Elsevier, p. 63-114.

Cox, K.G.; Bell, J.D. & Pankhurst, R.J. 1979. *The Interpretation of Igneous Rocks*. London, George, Allen and Unwin, 445p.

Cullers, R.L.; Yeh, L.T.; Chaudhury, S. & Guidotti, C.V. 1997. Rare earth elements in Silurian pelitic schists from NW Maine. *Geochimistry Cosmochimica Acta*, *38*: 389-400.

Ebert, H. 1958. *Discordâncias pré-cambrianas em Carandaí, Minas Gerais*. Rio de Janeiro, DNPM/DGM, 48p.

Hasui, Y. & Oliveira, M.A.F. 1984. Província Mantiqueira, Setor Central. *In*: ALMEIDA, F.F.M. & HASUI, H. (Eds.), *O Pré-Cambriano do Brasil*. São Paulo, Edgard Blucher, p. 308-344

Heilbron, M.; Pedrosa-Soares, A.C.; Campos Neto, M.; Silva, L.C.; Trouw, R.A.J. & Janasi, V.C. 2004. A Província Mantiqueira. *In*: MANTESSO-NETO, V.; BARTORELLI, A.; CARNEIRO, C.D.R. & BRITO NEVES, B.B. (Eds.), *O Desvendar de um Continente: A Moderna Geologia da América do Sul e o Legado da Obra de Fernando Flávio Marques de Almeida*. São Paulo, Beca, p. 203-234.

Hoffman, E.L. 1992. Instrumental Neutron Activation in Geoanalysis. *Journal of Geochemical Exploration*, *44*: 297-319.

Irvine, T.N. & Baragar, W.R. 1971. A guide to the chemical classification of the common igneous rocks. *Canadian Journal of Earth Sciences*, *8*: 523-548.

Kempton, P.D.; Harmon, R.S.; Hawkesworth, C.J. & Moorbath, S. 1990 Petrology and geochemistry of lower crustal granulites from the Geronimo volcanic field, southeastern Arizona. *Geochimica Cosmochimica Acta*, *54*: 3401-3426.

Machado Filho, L.; Ribeiro, M.W.; Gonzalez, S.R.; Schenini, C.A.; Santos Neto, A.; Palmeira, R.G.B.; Pires, J.L.; Teixeira, W. & Castro, H.E.F. 1983. *In*: MME, Projeto Radambrasil Folhas SF-23/24, Rio de Janeiro/Vitória,

Geologia, p. 27-304

Maniar, P. D. & Piccoli, P. M. 1989. Tectonic discrimination of granitoids. *Geological Society of America Bulletin*, 101: 635–643.

Meschede, M.1986. A method of discriminating between different types of mid-ocean ridge basalts and continental tholeiites with the Nb-Zr-Y diagram. *Chemical* Geology, 56: 207-218.

Mysen, B.O. & Kushiro, L. 1977. Compositional variations of coexisting phases with degree of melting of peridotite in the upper mantle. *American Mineralogist*, 62: 843-865.

Muecke, G.K.; Pride, C. & Sarkar, P. 1979. Rare-earth element geochemistry of regional metamorphic rocks. *Physics and Chemistry of the Earth*, 11: 449-464

Nogueira, J.R.; Choudhuri, A. & Trouw, R.A.J. 1999. Fluid inclusion studies, P-T-t paths and geotectonic evolution of the granulite facies terrain of Juiz de Fora, southeastern Brazil. *In*: MURTHY, N.G.K. & RAM-MOHAM., V. (Eds.), *Charnockite and Granulite Facies Rocks*. Madras, Geological Association of Tamil Nadu, p. 43-51.

Nogueira, J.R.; Almeida, J.C.H. & Toledo, C.L.B. 2003. Structural framework of the Ribeira Belt at the Juiz de Fora region, SE Brazil. *In*: INTERNATIONAL SYMPOSIUM ON TECTONICS, 3, Búzios, 2003, *Boletim de Resumos*, SBG, p. 163-165.

Pearce, T.H. 1968. A contribution to the theory of variation diagrams. *Contributions to Mineralogy and Petrology*, 19: 142-157

Pearce, J. A. & Cann, J. R.1973. Tectonic setting of basic volcanic rocks determined using trace element analyses. *Earth and Planetary Science Letters*, 19: 290-300.

Pearce, J.A. & Norry, M.J. 1979. Petrogenetic Implications of Ti, Zr, Y, and Nb Variations in Intrusive Rocks. *Contributions to Mineralogy and Petrology*, 69: 33-47.

Pearce, J.A.; Harris, N.B.W. & Tindle, A.J. 1984. Trace element discrimination diagrams for the tectonic interpretation of granitic rocks. *Journal of Petrology*, 25: 956-83.

Pedrosa-Soares, A.C. & Wiedemann-Leonardos, C.M. 2000. Evolution of the Araçuaí Belt and its connection to the Ribeira Belt, Eastern Brazil. *In*: CORDANI, U.; MILANI, E.; THOMAZ-FILHO, A. & CAMPOS, D.A (Eds.), *Tectonic Evolution of South America*. São Paulo, Sociedade Brasileira de Geologia, p. 265-285.

Pedrosa-Soares, A.C.; Noce, C.M.; Wiedemann, C. & Pinto, C.P. 2001. The Araçuaí-West-Congo Orogen in Brazil: An overview of a confined orogen formed during Gondwanaland assembly. *Precambrian Research*, 110: 307-323.

Peres, G.G.; Alkmim, F.F. & Jordt-Evangelista, H. 2004. The southern Araçuaí belt and the Dom Silvério Group: geologic architecture and tectonic significance. *Anais Academia Brasileira de Ciências*, 76: 771-790.

Rudnick, R.L.; McDonough, W.F.; McCulloch, M.T. & Taylor, S.R. 1986. Lower crustal xenoliths from Queensland, Australia: Evidence for deep crustal assimilation and fractionation of continental basalts. *Geochimica et Cosmochimica Acta, 50*: 1099- 1115.

Streckeisen, A. 1976. To each plutonic rock its proper name. *Earth Science Reviews, 4*: 1-33.

Silva, L.C.; Armstrong, R.; Noce, C.M.; Pimentel, M.M.; Pedrosa Soares, A.C.; Leite, C.; Vieira, V.S. & Paes, V.C. 2002. Reavaliação U-Pb SHRIMP em terrenos pré-cambrianos brasileiros. Parte II: Orógeno Araçuaí, Cinturão Mineiro e Cráton São Francisco Meridional. *Revista Brasileira de Geociências, 32*: 513-528

Thompson, R.N. 1982. Magmatism of the British Tertiary province. *Scottish Journal of Geology, 18*: 49-107.

Walter, M.J. & Presnall, D.C. 1994. Melting behavior of simplified lherzolite in the system CaO MgO Al2O3 SiO2 Na2O from 7 to 35 kbar. *Journal of Petrology, 35*: 329-359.